

The work is devoted to the description of the development of compression algorithms for hyperspectral aerospace images based on discrete orthogonal transformations for the purpose of subsequent compression in Earth remote sensing systems. As compression algorithms necessary to reduce the amount of transmitted information, it is proposed to use the developed compression methods based on Walsh-Hadamard transformations and discrete-cosine transformation. The paper considers a methodology for developing lossy and high-quality compression algorithms during recovery of 85 % or more, taking into account which an adaptive algorithm for compressing hyperspectral AI and the generated quantization table have been developed. The existing solutions to the lossless compression problem for hyperspectral aerospace images are analyzed. Based on them, a compression algorithm is proposed taking into account inter-channel correlation and the Walsh-Hadamard transformation, characterized by data transformation with a decrease in the range of the initial values by forming a set of channel groups [10–15] with high intra-group correlation [0.9–1] of the corresponding pairs with the selection of optimal parameters. The results obtained in the course of the research allow us to determine the optimal parameters for compression: the results of the compression ratio indicators were improved by more than 30 % with an increase in the size of the parameter channels. This is due to the fact that the more values to be converted, the fewer bits are required to store them. The best values of the compression ratio [8–12] are achieved by choosing the number of channels in an ordered group with high correlation

Keywords: hyperspectral aerospace images, compression algorithm, discrete transformations, compression ratio, discrete-cosine transformation, Walsh-Hadamard

Received date 25.06.2021

Accepted date 15.01.2022

Published date 25.02.2022

How to Cite: Sarinova, A., Dunayev, P., Bekbayeva, A., Mekhtiyev, A., Sarsikayev, Y. (2022). Development of compression algorithms for hyperspectral aerospace images based on discrete orthogonal transformations. *Eastern-European Journal of Enterprise Technologies*, 1 (2 (115)), 22–30. doi: <https://doi.org/10.15587/1729-4061.2022.251404>

1. Introduction

Modern satellite centers for space monitoring and remote sensing of the Earth (RSE) promptly receive, register, process, archive and distribute large amounts of data, sometimes amounting to hundreds of gigabytes. At the present stage of the development of science, hyperspectral AI is actively being investigated. Aerospace remote sensing images have various characteristics – spectral, radiometric, spatial resolutions, geometric dimensions of the scene. Hyperspectral AI RSE are important for observing and studying changes in the Earth's surface, monitoring natural resources and the consequences of emergencies, etc.

Thus, hyperspectral AI are characterized by three features: spectral resolution, number of channels and inter-channel correlation. These signs were studied separately, which suggests their interaction. Therefore, one of the key tasks in the field of remote sensing is the archiving of hyperspectral AI in order to increase the efficiency of data transmission over communication channels of limited bandwidth and their compression.

Currently, the development of software systems for the transmission of such data is an urgent task. In solving this problem, there are two areas of research: the development of compression algorithms used in ground-based remote sensing data reception and processing centers; the development of algorithms used onboard the spacecraft. Research is actively being conducted in the field of developing compression algorithms of the first direction, in which there are many publications. In the second direction of research, there is a potential for the development of algorithms dictated by the necessary list of problems to solve the compression problem, therefore this problem is relevant.

2. Literature review and problem statement

Hyperspectral aerospace images are necessary for monitoring natural resources and the consequences of emergencies, etc. In solving this problem, there are various areas of research in which research is actively conducted in the field

UDC 004.627

DOI: 10.15587/1729-4061.2022.251404

DEVELOPMENT OF COMPRESSION ALGORITHMS FOR HYPERSPECTRAL AEROSPACE IMAGES BASED ON DISCRETE ORTHOGONAL TRANSFORMATIONS

Assiya Sarinova

Corresponding author

PhD*

E-mail: assiya_prog@mail.ru

Pavel Dunayev

PhD

Department of Radio Engineering,
Electronics and Telecommunications**

Aigul Bekbayeva

MSc, Deputy Director

Center for Technological Competence in the Field of
Digitalization of Agro-Industrial Complex**

Ali Mekhtiyev

PhD, Professor*

Yermek Sarsikayev

PhD, Head of Department*

*Department of Operation of Electrical Equipment**

**S. Seifullin Kazakh Agro Technical University

Zhenis ave., 62, Nur-Sultan, Republic of Kazakhstan, 010011

of developing compression algorithms. Lossy compression algorithms and methods cover a wide range of compression. Among them, the most common are orthogonal and wavelet transformations, the JPEG compression algorithm.

Researchers are very interested in the methods of compression of aerospace images with losses, which give significant results in the efficiency of the compression ratio, the use of orthogonal transformations: discrete-cosine transformation (DCT), discrete wavelet transform (DWT), SPIHT, prediction, JPEG, JPEG2000 and at the last stage entropy coding. Here are some compression methods and algorithms that have significant research results.

The paper [1] presents the results of the research. An algorithm based on the third order of the interchannel predictor and the inverse pixel search scheme is proposed. In particular, an adaptive algorithm of step-by-step search and a modified spatio-spectral predictor is proposed, which is able to capture most of the correlation by performing a search twice in the current range. Channels are divided into groups depending on the correlation coefficient of adjacent channels, and then, the reordering algorithm is applied to each group. The prediction method uses the similarity of structures and the ratio of pixels between two adjacent spectral channels and is further encoded by adaptive arithmetic coding. The proposed compression scheme produces an average compression ratio of 3.92.

The paper [2] presents the results of research that improved Shapiro's EZW algorithm. Hybrid transformations consist in the Karhunen-Loève Transform (KLT), which decode the spectral data of hyperspectral aerospace images, and DWT is applied to spatial data. The proposed image compression has a compression ratio of 7.9. Disadvantages: wavelet coefficients can be scanned earlier than others in low-level subchannels; the basis of the encoder is the EZW Shapiro algorithm, encoding residual values and implementing only the dominant block; the algorithm is complicated by numerical efficiency.

Researchers [3] investigated the compression of hyperspectral AI using the 3D SPIHT algorithm. At the first stage, 3D Fiberboard is used, at the second stage, 3D-SPIHT is encoded by the algorithm, where there is a significant correlation between different channel ranges. After decompression, the images are evaluated using the PSNR algorithm. The compression base of the PREP and SPIHT provides a high compression ratio. Disadvantage: the algorithm can be implemented for any image size, the image size proportionally increases the time required for image compression and restoration, which increases the computational complexity of the algorithm.

For example, [4] presents approaches to lossless compression of hyperspectral AI using adaptive prediction and reverse-search schemes. The proposed scheme is based on the prediction approach and uses two new approaches to improve compression performance. The first approach uses spatial correlation of data and formulates the output of spectral prediction in the Winner filtering process. In the second approach, the search scheme is used instead of reference tables, which significantly reduces the need for memory. The search is significantly reduced using the quantization index. The compression scheme proposed by the researchers consists of five main modules: internal prediction, inter-/multispectral prediction, search index (BSI), quantization index and entropy coding. The proposed scheme supports intra- and inter-band prediction, taking into account the properties of

hyperspectral images, prediction is performed in the spectral region. The proposed lossless compression schemes produce an average compression ratio reaching 3.85, the best result among the compared schemes.

The fast Walsh-Hadamard transformation algorithm based on a system of functions and their properties is used in signal and image processing. Scientists [5] investigated the compression of hyperspectral aerospace images using DVP and Walsh-Hadamard transformation (WHT). A hybrid technology called Walsh wavelet transformation is proposed, consisting of four stages. At the first stage, two levels of fiberboard are applied, at the second stage, 2D-UAP are applied on each block of the low-frequency range ($N=4$). At the third stage, finding the values from the transformed sub-images of each range, then they are compressed by arithmetic coding, this is the fourth stage. This technology provides a small compression ratio of 1.8.

The paper [6] deals with the compression and classification of hyperspectral images using the Discrete Wavelet Technique in conjunction with Non-negative Tucker Decomposition. This algorithm exploits both the spectral and the spatial information of the images. The core idea behind the proposed technique is to apply TD on the DWT coefficients of spectral bands of HSIs. The results obtained by using the proposed method gives a satisfactory performance in terms of PSNR (Peak signal-to-noise ratio). The disadvantage of the method is that the computational load of the proposed method is high, i. e. it is necessary to reduce the calculation of the main tensor.

DCT and SPIHT are the most widely used methods of hyperspectral image compression. In [7], a DCT-based DSC technique was carried out using arithmetic code to evaluate their performance on hyperspectral images. DCT-based DSCs using arithmetic code were investigated using Samson hyperspectral sample data. The performance of these algorithms is estimated based on the PSNR of the compressed image and the compression ratio. PSNR=42.66152 dB, CR=48 % of MSE, it is observed that the difference between the original and the restored image is very small. Therefore, it can be concluded that the quality suffers and it is necessary to pre-process images before converting and compressing them.

In [8], principal component analysis (PCA) to the compression of hyperspectral AI was applied. The hybrid compression method (DVP-TD) was used, which was effective because it provided detailed information about the spectral ranges of the image. DVP-TD using "global" encoding achieves a higher value of the peak signal-to-noise ratio (PSNR), shorter execution time and a high compression ratio of 8.0. The main disadvantage is that the PCA covariance matrix, which is used for decorrelation among frequency bands, should already be calculated, and therefore depends on the data. Therefore, it is necessary to reduce the computational load of the proposed method.

In [9], when studying the compression of hyperspectral AI, the requirements for an accurate assessment of image quality are given, the process of data collection and compression properties (data quality) are considered. The authors divide compression methods into three groups: prediction, vector quantization and encoding with transformation. Encoding with transformation is implemented in three steps: the first step is to transform the data into an area where the representation of the data is more compact and less correlated; the second step is to encode this information in as efficient quality as possible; in the last step of encoding, information loss occurs through quantization.

The paper [10] considers the technique of channel rearrangement and their search makes it possible to determine a group of channels that are highly correlated with each other. However, studies have shown that the process of calculating the spectral correlation matrix takes a lot of time.

The same approach is implemented in [11]. The technique of regrouping channels and their search allows determining a group of bands that are highly correlated with each other. The proposed predictor has a better performance than the methods listed in the table. The improvement of the number of bits per pixel per channel is reduced using a prediction algorithm. The main disadvantage of this method is that it depends on the calculation of the spectral correlation matrix, which is a time-consuming process.

For example in [12], a group of researchers believe that the wavelet transform is one of the current trends in new compression algorithms for hyperspectral AI. The use of wavelets provides a progressive compressed bitstream, which allows achieving compression without loss of quality with minimal loss of information. The advantage is provided by the use of entropy coding compression. Disadvantages may be: partially preserved lossy compression performance; increased complexity of the algorithm in terms of the required RAM; relatively low quality with intermediate wavelet transformations.

In [13], the research uses a predictive model on AVIRIS images by individualizing, using an autonomous approach, a common subset of bands that are not spectrally related to any other bands. The main result of this work is a list of bands unrelated to others for AVIRIS images. The clustering trees obtained for AVIRIS and the relationship between the bands they depict are also an interesting starting point for future research. This approach needs to be improved to make it more reliable, and the development of other approaches that aim to improve lossless compression of hyperspectral images with reduced complexity of the compression algorithm, even with different types of hyperspectral images.

The letter [11] proposes a new lossless hyperspectral image compression algorithm using hybrid contextual prediction. Lossless compression algorithms are usually divided into two stages: the decorrelation stage and the encoding stage. The decorrelation stage supports both in-band and inter-band predictions. In-band (spatial) prediction uses the median prediction model because the median predictor is fast and efficient. Interband prediction uses hybrid contextual prediction. The results of the study show that the algorithm provides low compression coefficients of 3, 19 with low complexity and computational costs.

Attempts have been made [14], a multi-stage algorithm has been proposed, including accounting for inter-band correlation and preliminary byte processing of data, which allows to significantly (up to 46 %) increase the degree of data compression compared to analogs. A three-stage algorithm for compressing multispectral aerospace images based on the use of the wavelet transform and taking into account the interband dependence is proposed. The research results have shown the superiority of the proposed algorithm to varying degrees over analogs in compression with more significant computational costs. The works of the authors of this study with Walsh-Hadamard transformations in comparison with the discrete-cosine transformation have not been investigated in previous works of the authors.

Based on the above studies of hyperspectral AI in the field of compression presented in the works of scientists from

Russia, China, the USA, India, etc., it can be assumed that the developed lossless compression methods and algorithms for hyperspectral AI can be improved by reducing their computational efficiency and increasing the compression ratio due to significant preprocessing steps. In addition, new stages of compression preprocessing can be proposed on the example of Walsh-Hadamard in comparison with discrete-cosine transformation, which effectively increase the compression ratio and reduce the time of forward and reverse transformations.

3. The aim and objectives of the study

The aim of this work is to describe a compression algorithm taking into account inter-channel correlation, characterized by the Walsh-Hadamard transformation of data with a decrease in the range of the initial values by forming a set of channel groups with high intra-group correlation of the corresponding pairs with the selection of optimal parameters. Improving and obtaining an effective result of compression of hyperspectral aerospace images can be achieved by performing the following objectives:

- to develop a new method to account for inter-channel correlation in the form of selecting the number of channels by grouping them and selecting the best correlated channel that determines the compression sequence;
- to produce Walsh-Hadamard difference transformations obtained by forming channel groups, which will allow storing data with lower bit depth and excellent quality, depending on the selected quantization coefficient;
- to develop a transformation method in which the range of values of the original hyperspectral image will be changed by forming additional data structures that are effectively compressed using entropy coding in comparison with the Walsh-Hadamard transform and the discrete-cosine transform.

4. Materials and methods

4.1. Proposed methods and algorithms for processing hyperspectral aerospace images

One of the popular graphic formats designed for image storage is the JPEG algorithm, which allows lossy and lossless image compression. Let's consider the algorithm of operation of a variety of the simplest lossy JPEG encoder, the process of which consists of the following stages, Fig. 1:

1. Preprocessing – preprocessing of an image, leading it to a convenient representation for subsequent encoding.
2. The DCT is used by the JPEG encoder to transform the image from its spatial representation to the spectral one.
3. Quantization is the stage at which the main loss of information occurs due to the rounding of non-essential, high-frequency DCT coefficients.
4. Compression is the encoding of the received data by entropy algorithms (arithmetic coding, Huffman algorithm, etc.)

An important step in the JPEG algorithm is the DCT, which is a kind of Fourier transform. If we consider the image as a set of spatial waves, where the X and Y axes correspond to the width and height of the image, and the Z axis corresponds to the color values of the corresponding pixels, then we can move from the spatial representation of the image to its spectral representation and vice versa [33, 44, 53].

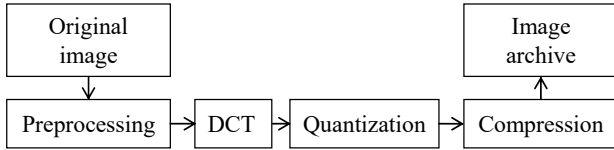


Fig. 1. Stages of operation of the JPEG encoder

The analysis of existing and separately developed algorithms and methods of compression of hyperspectral AI with losses allows us to determine the main directions of research in the field of the construction of effective compression algorithms for solving the problem of compression and application in the processing of hyperspectral AI:

- discrete transformations;
- wavelet and orthogonal transformations;
- evaluation of the quality criteria of the reconstructed images using quality metrics PSNR, MSE, PMSE, etc.;
- at the stage of compression of the resulting transformations: adaptive arithmetic coding and Huffman algorithm.

An algorithm and sequence of preprocessing with Walsh-Hadamard transformation of hyperspectral AI are proposed.

4. 2. Walsh-Hadamard transformation

Algorithms for processing hyperspectral AI with losses based on discrete transformations have been developed. The sequence of stages is as follows:

1. Transformation of the data structure based on the original hyperspectral AI, coefficient values, based on Walsh-Hadamard three levels.
2. The original transformation of the data structure based on the original hyperspectral AI, storing the values of the coefficients, based on the discrete-cosine transformation with the generated quantization table.
3. Transformation of the obtained data structures based on steps 1–2 by means of the generated coefficient quantization table.
4. Using standard criteria for the quality of restored images.
5. Compression of the obtained structures of stage 4 by one of the standard entropy algorithms.
6. Experimental study of conversion algorithms by compression ratio and quality of recovered data.

Let’s look at the stages of the algorithms in more detail.

For a step-by-step description of the transformation, it is necessary to introduce the following objects into consideration:

- the source image is the matrix of image values $I[m, n, k]$, where m, n, k are the indexes of rows, columns and channels of the source image, $m=1, 2, \dots, M, n=1, 2, \dots, N, k=1, 2, \dots, K$;
- the WHT transformation is filters that divide images into low-frequency and high-frequency components (to get the original image, you need to combine the components again);
- spectral component (SC) is the spectral component of the matrix $I[m, n, k]$.

Consider an example of the Walsh-Hadamard transformation (WHT) for a fragment of hyperspectral AI.

Let the fragment of AI represent a matrix consisting of m rows, n columns and k channels: $I[m, n, k]=I[10, 10, 10]$.

The direct transformation of WHT is presented in the matrix form of H_{wt2} , a fragment of AI is taken (123, 105, 121, 103, 118, 100, 123, 123, 122, 104), i. e.

$$H_{wt2} \cdot I[m, n, k] = H'_{wt2}[SC].$$

The WHT transform is filters that divide an image into low-frequency and high-frequency components. To get the original image, you just need to combine these components again. An example of direct conversion of hyperspectral aerospace images is presented below.

$$\begin{pmatrix} \frac{1}{2} & \frac{1}{2} & 0 & 0 & 0 & 0 & 0 & 0 & 0 & 0 \\ \frac{1}{2} & -\frac{1}{2} & 0 & 0 & 0 & 0 & 0 & 0 & 0 & 0 \\ 0 & 0 & \frac{1}{2} & \frac{1}{2} & 0 & 0 & 0 & 0 & 0 & 0 \\ 0 & 0 & \frac{1}{2} & -\frac{1}{2} & 0 & 0 & 0 & 0 & 0 & 0 \\ 0 & 0 & 0 & 0 & \frac{1}{2} & \frac{1}{2} & 0 & 0 & 0 & 0 \\ 0 & 0 & 0 & 0 & \frac{1}{2} & -\frac{1}{2} & 0 & 0 & 0 & 0 \\ 0 & 0 & 0 & 0 & 0 & 0 & \frac{1}{2} & \frac{1}{2} & 0 & 0 \\ 0 & 0 & 0 & 0 & 0 & 0 & \frac{1}{2} & -\frac{1}{2} & 0 & 0 \\ 0 & 0 & 0 & 0 & 0 & 0 & 0 & 0 & \frac{1}{2} & \frac{1}{2} \\ 0 & 0 & 0 & 0 & 0 & 0 & 0 & 0 & \frac{1}{2} & -\frac{1}{2} \end{pmatrix} *$$

$$\begin{matrix} [123] \\ 105 \\ 121 \\ 103 \\ 118 \\ 100 \\ 123 \\ 123 \\ 122 \\ 104 \end{matrix} = \begin{matrix} \left[\begin{matrix} \frac{123}{2} + \frac{105}{2} \\ \frac{123}{2} - \frac{105}{2} \\ \frac{121}{2} + \frac{103}{2} \\ \frac{121}{2} - \frac{103}{2} \\ \frac{118}{2} + \frac{100}{2} \\ \frac{118}{2} - \frac{100}{2} \\ \frac{123}{2} + \frac{123}{2} \\ \frac{123}{2} - \frac{123}{2} \\ \frac{122}{2} + \frac{104}{2} \\ \frac{122}{2} - \frac{104}{2} \end{matrix} \right] = \begin{matrix} \left[\begin{matrix} \frac{228}{2} \\ \frac{18}{2} \\ \frac{224}{2} \\ \frac{18}{2} \\ \frac{218}{2} \\ \frac{18}{2} \\ \frac{246}{2} \\ 0 \\ \frac{226}{2} \\ \frac{18}{2} \end{matrix} \right] \end{matrix}$$

As a result, after such a transformation, we obtain the coefficients of the low-frequency and high-frequency components of the $SC=114, 9, 112, 9, 114, 9, 123, 0, 123, 9$. During quantization, high-frequency coefficients (close to zero and negative values) are rounded to zero.

It should be noted that the H_{wt4} and H_{wt8} level matrices are calculated in the same way as H_{wt2} .

At the stage of restoring the original image channels, decoding occurs.

$$H_{wt2}^T \cdot H'_{wt2}[SC] = I[m, n, k],$$

where H_{wt2}^T – inverse wavelet transform WHT, $H'_{wt2}[SC]$ – spectral component.

An example of the reverse transformation is presented as follows:

$$\begin{pmatrix} \frac{1}{2} & \frac{1}{2} & 0 & 0 & 0 & 0 & 0 & 0 & 0 & 0 \\ \frac{1}{2} & -\frac{1}{2} & 0 & 0 & 0 & 0 & 0 & 0 & 0 & 0 \\ 0 & 0 & \frac{1}{2} & \frac{1}{2} & 0 & 0 & 0 & 0 & 0 & 0 \\ 0 & 0 & \frac{1}{2} & -\frac{1}{2} & 0 & 0 & 0 & 0 & 0 & 0 \\ 0 & 0 & 0 & 0 & \frac{1}{2} & \frac{1}{2} & 0 & 0 & 0 & 0 \\ 0 & 0 & 0 & 0 & \frac{1}{2} & -\frac{1}{2} & 0 & 0 & 0 & 0 \\ 0 & 0 & 0 & 0 & 0 & 0 & \frac{1}{2} & \frac{1}{2} & 0 & 0 \\ 0 & 0 & 0 & 0 & 0 & 0 & \frac{1}{2} & -\frac{1}{2} & 0 & 0 \\ 0 & 0 & 0 & 0 & 0 & 0 & 0 & 0 & \frac{1}{2} & \frac{1}{2} \\ 0 & 0 & 0 & 0 & 0 & 0 & 0 & 0 & \frac{1}{2} & -\frac{1}{2} \end{pmatrix} * \begin{pmatrix} \frac{228}{2} & \frac{228}{2} + \frac{18}{2} \\ \frac{18}{2} & \frac{228}{2} - \frac{18}{2} \\ \frac{224}{2} & \frac{224}{2} + \frac{18}{2} \\ \frac{18}{2} & \frac{224}{2} - \frac{18}{2} \\ \frac{218}{2} & \frac{218}{2} + \frac{18}{2} \\ \frac{18}{2} & \frac{218}{2} - \frac{18}{2} \\ \frac{246}{2} & \frac{246}{2} + 0 \\ 0 & 0 \\ \frac{226}{2} & \frac{226}{2} + \frac{18}{2} \\ \frac{18}{2} & \frac{226}{2} - \frac{18}{2} \\ \frac{2}{2} & \frac{2}{2} \end{pmatrix} = \begin{pmatrix} \frac{246}{2} \\ \frac{210}{2} \\ \frac{242}{2} \\ \frac{206}{2} \\ \frac{236}{2} \\ \frac{200}{2} \\ \frac{246}{2} \\ 0 \\ \frac{246}{2} \\ \frac{208}{2} \\ \frac{2}{2} \end{pmatrix}$$

By changing the basis of the matrix (H_4, H_8) with each submatrix, we perform a forward and reverse calculation, according to which each element of the transformed submatrix is calculated by the formulas:

$$WHT = \frac{\sum_{i=1}^n \mathbf{I}[m,n,k] \times H_w[i,j]}{2^H},$$

$$WHT_D = \sum_{i=1}^n \mathbf{I}[m,n,k] \times H_w[i,j] \times H,$$

where n – dimension of the Hadamard matrix, $\mathbf{I}[m,n,k]$ – a submatrix of the original matrix,

H_w – Hadamard matrix, i – the string of the current value in the submatrix, j – the column of the current value in the submatrix, H – matrix basis.

The advantage of the Walsh-Hadamard transform is the increased ability to detect low-frequency components due to the separation of hyperspectral AI channel regions into sublevels and the generated quantization coefficient.

4.3. Discrete-cosine transformation with generation of quantization tables

DCT is a transformation whose linear combination consists of known basis vectors weighted with n coefficients leading to the original vector.

Let's consider step-by-step transformation of hyperspectral AI channels using DCT.

1. Divide it into s blocks of pixels of size $n \times n$ (usually 8×8).
2. Apply DCT to each block, represent each block as a linear combination of 64 basic blocks.
3. All s vectors ($i=1, 2, \dots, s$).
4. Generation of the quantization table.

At the first step, as a result of the DCT conversion, two filters were built – high-frequency and low-frequency.

For low-frequency and high-frequency filters, we introduce some notation:

- DC – operator for the low-frequency filter;
- AC – operator for the high-frequency filter.

The figure below shows a fragment of the original hyperspectral aerospace image before the DCT transformation (Fig. 2). For visualization of matrices (hyperspectral image channels), a program was developed for Visual Studio 2017 (C#), which demonstrates the exact absolute values in digital form.

Based on the visible values, an algorithm of discrete-cosine transformation was proposed, applied specifically to hyperspectral images, since their structure differs from the usual image (picture). It was also revealed from previous studies by the authors [14] that channels close to each other have a high correlation of the values of the channel matrices, and this was used for further effective image compression after the DCT conversion.

In the scientific literature, DCT is a transformation whose linear combination consists of known basis vectors weighted with n coefficients leading to the original vector. The known basic transformation vectors from this class are “sinusoidal”, which means that they can be represented by sinusoidal waves or strongly localized in the frequency spectrum. The two-dimensional transformation of DCT follows the rectilinear form of the one-dimensional DCT. Let's use a two-dimensional DCT, formulas:

$$D_{ij} = \frac{1}{\sqrt{2h}} c_i c_j \sum_{z=0}^{h-1} \sum_{y=0}^{h-1} \mathbf{I}_{mn} \cos\left(\frac{(2n+1)j\pi}{2h}\right) \cos\left(\frac{(2m+1)i\pi}{2h}\right).$$

| | | | | | | | |
|------|------|------|------|------|------|------|------|
| 5498 | 5293 | 5096 | 5036 | 4924 | 4942 | 5464 | 5507 |
| 5303 | 5165 | 5123 | 4926 | 4960 | 4848 | 5183 | 5568 |
| 5096 | 5062 | 4942 | 4847 | 4967 | 4830 | 4882 | 5113 |
| 5209 | 5115 | 4926 | 4866 | 4849 | 4798 | 4960 | 5235 |
| 5114 | 5088 | 4994 | 4934 | 4831 | 4763 | 4917 | 5345 |
| 4958 | 5027 | 5010 | 4950 | 4907 | 4795 | 4770 | 4924 |
| 4968 | 5114 | 4994 | 4943 | 4951 | 4823 | 4806 | 4891 |
| 4840 | 4806 | 4831 | 4951 | 4917 | 4865 | 4728 | 4780 |

Fig. 2. The original data of a fragment of hyperspectral AI

By $0 \leq i, j \leq h-1$. It is divided into blocks of pixels $\mathbf{I}_{m,n}$ of size $h \times h$ (in our fragment $h=8$), used to find coefficients for each pixel block D_{ij} .

First, the rows of this block are considered using the transformation set by the internal sum

$$D_{m,j} = C_i \sum_{y=0}^{h-1} \mathbf{I}_{m,n} \cos\left(\frac{(2n+1)j\pi}{2h}\right).$$

The result of this rotation is a block $D_{m,j}$ of $h \times h$ coefficients, in which the first elements predominate in the rows, and all other elements are small. The external sum is equal to

$$D_{i,j} = \frac{1}{\sqrt{2h}} C_i \sum_{m=0}^{h-1} \mathbf{I}_{m,n} D_{m,n} \cos\left(\frac{(2m+1)i\pi}{2h}\right).$$

The result is one large coefficient in the upper left corner of the block and h^2-1 small coefficients in the remaining values. This interpretation considers a two-dimensional DCT as two different rotations of dimension n .

The second interpretation (by $h=8$) is to create 64 blocks of 8×8 values in each. All 64 blocks are considered as the basis of a 64-dimensional vector space (hyperspectral image channels). Any block of 8×8 can be expressed as a linear combination of these basic images, and all 64 weights of this linear combination form DCT coefficients.

After the DCT transformation, the fragment of hyperspectral AI has the following values, Fig. 3.

It can be seen from Fig. 1 that the high values of the conversion coefficients are concentrated in the upper left corner and only a small number of low-frequency coefficients prevail over the main ones. This allows you to reduce the values at the next stages of compression. The second step is the process of generating quantization tables. Quantization is performed as follows:

1. The arithmetic mean $I_{average}$ was calculated from all the values of the file.

2. To select the numerical quantization index $Quant$, the number for quantization was calculated, $Quant = \text{quantValue} \times I_{average} / 100$. For example, the numerical quantization index: $I_{average} \times 95 \% = 285 = Quant$. At the same time, the DC coefficients remain intact. For each hyperspectral AI channel, its own quantization table is generated.

For the above fragment of hyperspectral AI, the matrix after quantization is shown, Fig. 4. The quantization process is key in the compression process, the advantage of representation in the frequency domain lies in the visual quality of the reconstructed images. As a result, after quantization, most of the coefficients are zero.

As a result, most of the zeros will be placed at the end of the data compression stream. This stream with many consecutive zeros at the end of the block is optimized to achieve high compression in the entropy coding of the adaptive Huffman algorithm.

To determine the effectiveness of the proposed algorithm, a number of experiments were conducted on hyperspectral AI (hyperspectral Headwall Nano Hyperspec camera). The proposed algorithm is also compared with the experimental

results obtained for the universal compression algorithms of WinRAR, WinZip archivers and Lossless JPEG 2000 compression using an extension of the JPEG compression standard widely used in commercial remote sensing data processing systems (Table 1).

| | | | | | | | |
|-------|------|------|------|-----|------|-----|-----|
| 40008 | 204 | 708 | -320 | 268 | -139 | -51 | 51 |
| 799 | -176 | 654 | -84 | 60 | 89 | -57 | 114 |
| 188 | -64 | -79 | 102 | -64 | 137 | -55 | 26 |
| 326 | 29 | 157 | -119 | -47 | 79 | -56 | -1 |
| 97 | -94 | 173 | 25 | 44 | 129 | -26 | -63 |
| 33 | 128 | -9 | 118 | -91 | 14 | -96 | -12 |
| -207 | 41 | -198 | 118 | -28 | 34 | 1 | -18 |
| 13 | -1 | -3 | -14 | -2 | -35 | -20 | -11 |

Fig. 3. The coefficients obtained after the DCT conversion

| | | | | | | | |
|-------|---|-----|------|-----|---|---|---|
| 40008 | 0 | 708 | -320 | 268 | 0 | 0 | 0 |
| 799 | 0 | 654 | 0 | 0 | 0 | 0 | 0 |
| 0 | 0 | 0 | 0 | 0 | 0 | 0 | 0 |
| 326 | 0 | 0 | 0 | 0 | 0 | 0 | 0 |
| 0 | 0 | 0 | 0 | 0 | 0 | 0 | 0 |
| 0 | 0 | 0 | 0 | 0 | 0 | 0 | 0 |
| 0 | 0 | 0 | 0 | 0 | 0 | 0 | 0 |
| 0 | 0 | 0 | 0 | 0 | 0 | 0 | 0 |

Fig. 4. Generated quantization table after DCT

Table 1

Characteristics of test hyperspectral images

| Number of channels | Image size | Size (bytes) |
|--------------------|------------|--------------|
| 100 | 100×100 | 4,080,400 |
| 100 | 200×200 | 16,160,400 |
| 100 | 300×300 | 36,240,400 |
| 100 | 400×400 | 64,320,400 |
| 100 | 614×512 | 125,747,200 |
| 150 | 100×100 | 6,120,600 |
| 150 | 200×200 | 24,240,600 |
| 150 | 300×300 | 54,360,600 |
| 150 | 400×400 | 96,480,600 |
| 150 | 614×512 | 188,620,800 |
| 200 | 100×100 | 8,160,800 |
| 200 | 200×200 | 32,320,800 |
| 200 | 300×300 | 72,480,800 |
| 200 | 400×400 | 128,640,800 |
| 200 | 614×512 | 251,494,400 |
| 270 | 100×100 | 9,140,096 |
| 270 | 200×200 | 36,199,296 |
| 270 | 300×300 | 81,178,496 |
| 270 | 400×400 | 144,077,696 |
| 270 | 614×512 | 281,673,728 |

The experiments were performed on a PC with an Intel Core i5 2.29 GHz processor and 4 GB of RAM running the Windows 8.1 operating system.

5. Results of research of the parameters of the Walsh-Hadamard transformation and compression of hyperspectral images

5.1. Comparative results of experiments on the number of channels

Studies have been carried out on the indicators of compression degrees in the context of the number of channels of hyperspectral images of orthogonal Walsh-Hadamard transformations, DCT and JPEG 2000 with losses shown in Fig. 5. It is shown that DCT prevails over Walsh-Hadamard transformations and JPEG with losses in compression ratio with high quality of restored images, where K is the number of hyperspectral image channels, D – compression ratio.

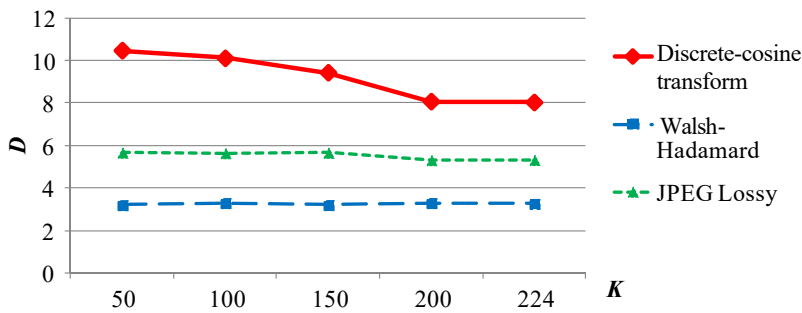


Fig. 5. Compression algorithms D from K

As can be seen from Fig. 5, the indicators of the degrees of compression of the DCT with losses are superior in the degree of compression of the Walsh-Hadamard transformation and the JPEG Lossy compressor.

5.2. Comparative results of experiments on the selected quantization coefficient with high quality and minimal loss

Fig. 6 shows the results of the Walsh-Hadamard transform, discrete-cosine transform, discrete wavelet transform and JPEG Lossy algorithm at different loss levels in %, from which it can be seen that with increasing quantization coefficient, the compression ratio increases. Conversion algorithms by compression ratio D and loss level P (in percent) with the number of hyperspectral image channels=100.

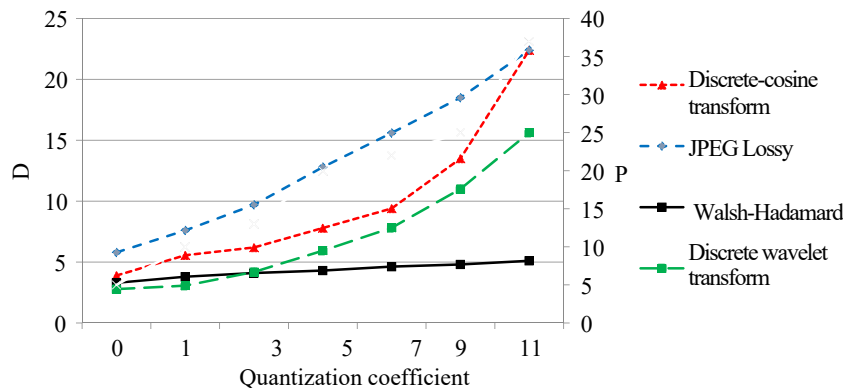


Fig. 6. Dependences of $Quant$ on D, P

Indicators of the quality metrics of the restored images were determined using $PSNR$ and MSD . The degree of distortion compares the ratio between compression and distortion in lossy algorithms. The score is defined as the average of the number of bits needed to represent each pixel. Measured in bits per pixel (bpp – bits per pixel). Distortion is usually measured using $PSNR$.

5.3. Comparative results of the dependence of the compression ratio on the quality of restored images

For the transformations of clauses 4.2, 4.3, criteria for evaluating the quality of reconstructed images when compressing hyperspectral AI with losses are given, comparative characteristics of compression performance in terms of peak signal-to-noise ratio ($PSNR$) are carried out.

Consider the calculation of $PSNR$ in detail:

Let's introduce some additional notation:

– standard deviation (SD);

– arrays of recovered images $\hat{I}_{m,n}$;

– one-dimensional arrays $\mathbf{I}'_{MSE}[m,n,k]$;

– one-dimensional arrays $\mathbf{I}'_{PSNR}[m,n,k]$.

Step 1. Calculate the matrix based on the original and reconstructed images to calculate the standard deviation:

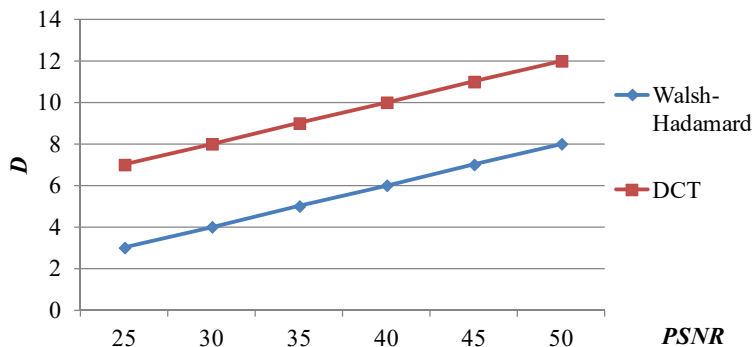
$$SD = \frac{\sum_{m=1}^M \sum_{n=1}^N (I_{m,n} - \hat{I}_{m,n})^2}{M \cdot N},$$

where $I_{m,n}$ – meaning m, n – pixels of the original image, $\hat{I}_{m,n}$ – corresponds to the value m, n – pixels of the restored image, M, N – image dimensions. We will save the results in a one-dimensional array $\mathbf{I}'_{MSE}[m,n,k]$.

Step 2. Calculate the mean square deviation, $PSNR$: $PSNR = 10 \lg_{10}(\max[I_{m,n}]^2 / MSE)$. We will put the results in a one-dimensional array $\mathbf{I}'_{PSNR}[m,n,k]$.

Fig. 7 shows the dependence of $PSNR$ on the compression ratio D for DCT and the Walsh-Hadamard transformation.

The results of the study show a high degree of compression with minor quality losses of the Walsh-Hadamard transform and the discrete-cosine transform, so $PSNR$ lies in the range of 25–50. This allows us to say about the effectiveness of these stages of the Walsh-Hadamard transformation and the discrete-cosine transformation in the application of hyperspectral image compression.

Fig. 7. Dependence of PSNR on D

6. Discussion of experimental results of transformations and compressions of hyperspectral images using various stages of the Walsh-Hadamard transformation and discrete-cosine transformation

At the end of the research, it was noted that the efficiency in the compression ratio is achieved by applying the proposed compression algorithm, taking into account the correlation and ordering of channel groups and transformation based on discrete-cosine and Walsh-Hadamard. The results of experiments and studies show that this algorithm finds the best pairs of correlated channels than without ordering (with the selected reference channel), while achieving a high degree of compression and minimal loss of quality of the restored aerospace images.

The following conclusions should be drawn from the conducted studies:

- the compression algorithm based on orthogonal discrete-cosine and Walsh-Hadamard transformations (Fig. 3, 4), taking into account the inter-band correlation, allows increasing the compression ratio to ($D > 8$) compared to universal archivers and the JPEG Lossy algorithm (Fig. 5). Unlike [5, 6, 8, 9], the advantages of this algorithm are that subtraction (difference transformation) is effective when selecting a large range of channels in a group, then the average values of differences will be the smallest, which will allow storing in the smallest amount on disk than with a small number of K in N , where $N [2:10]$:

- the proposed approach to the formation and ordering of a set of channel groups with high intra-group correlation has increased the effectiveness of the channel subtraction stage (difference transformation), Fig. 6. In contrast to the studies [1–3], thanks to the proposed algorithm, the best values of the compression ratio are achieved by choosing the number of channels in an ordered group, at $15 > K > 10$ and taking into account the inter-channel correlation of the parameter, the Cog shows the highest values in the compression ratio of the channel number, at $170 > N > 0$;

- the obtained results of comparing the transformed hyperspectral AI with archivers and JPEG 2000 Lossless allow us to assert the effectiveness of the indexed conversion method (Fig. 7). In contrast to [4, 7], thanks to the use of the channel subtraction stage (difference transformation) after the Walsh-Hadamard transformation and DCT, the compression ratio indicators were achieved at

$D[8:12]$ and the quality of the restored images with a loss percentage of 85 or more was achieved.

The limitations of this study may be related to the amount of data being compressed and the recovery time of the original images, and more powerful computing resources and occupied hard disk space may be required.

The prospects for further research may be the compression of hyperspectral images by an adaptive algorithm using regression analysis, a new model for accounting for interchannel correlation based on block-by-block transformation (SPIHT), as well as a decrease in computational efficiency. The disadvantage of the study is small computing resources for larger amounts of data.

7. Conclusions

1. An algorithm based on discrete transformations, especially Walsh-Hadamard, has been developed, which allows increasing the compression ratio of hyperspectral images to $R=8$, which is higher compared to analogs due to difference subtraction with small losses of restored images at a percentage of 85 or more. Thanks to the pre-processing of the hyperspectral image, which leads it to a convenient representation for subsequent encoding, high compression coefficients have been achieved compared to previous studies.

2. An approach to lossy compression of hyperspectral images has been developed, defined in adaptive and difference transformations based on the Walsh-Hadamard transform, the discrete-cosine transform and the generated quantization table, while the $PSNR$ lies in the 30–50 range, the percentage of quality of the restored images is preserved up to 85%. The result is achieved thanks to the quantization table and its parameters, where $Quant=5$. This means rounding the values of the original image after transformations to a loss level of only 5%, so the quality of the restored images varies from 85% or more.

3. The results of comparing the transformed hyperspectral image using the obtained quantization coefficients are developed and obtained, which indicate the effectiveness of using discrete-cosine transformations with adaptive Huffman coding. Adaptive coding of the Huffman algorithm after Walsh-Hadamard transformations and DCT, which generates an intuitive program code table, has been developed and proposed. This modification made it possible to increase the degree of compression of hyperspectral images due to the analysis of the frequencies of channel pairs, since codes of shorter length are allocated to more common values.

Acknowledgments

This work was carried out within the framework of the IRN research project Grant No. AP09561922 “Development of a mathematical apparatus for the use of hyperspectral images for phytosanitary inspection of grain crops during aerospace survey”.

References

1. Li, C., Guo, K. (2014). Lossless Compression of Hyperspectral Images Using Three-Stage Prediction with Adaptive Search Threshold. *International Journal of Signal Processing, Image Processing and Pattern Recognition*, 7 (3), 305–316. doi: <https://doi.org/10.14257/ijcip.2014.7.3.25>
2. Cheng, K.-J., Dill, J. C. (2014). An Improved EZW Hyperspectral Image Compression. *Journal of Computer and Communications*, 02 (02), 31–36. doi: <https://doi.org/10.4236/jcc.2014.22006>
3. Puri, A., Sharifahmadian, E., Latifi, S. (2014). A Comparison of Hyperspectral Image Compression Methods. *International Journal of Computer and Electrical Engineering*, 6 (6), 493–500. doi: <https://doi.org/10.17706/ijcee.2014.v6.867>
4. Lin, H.-C., Hwang, Y.-T. (2011). Lossless Compression of Hyperspectral Images Using Adaptive Prediction and Backward Search Schemes. *Journal of Information Science and Engineering*, 27, 419–435. Available at: <https://citeseerx.ist.psu.edu/viewdoc/download?doi=10.1.1.429.9325&rep=rep1&type=pdf>
5. Sujithra, D. S., Manickam, T., Sudheer, D. S. (2013). Compression of hyperspectral image using discrete wavelet transform and Walsh Hadamard transform. *International journal of advanced research in electronics and communication engineering (IJARECE)*, 2 (3), 314–319. Available at: <http://ijarece.org/wp-content/uploads/2013/08/IJARECE-VOL-2-ISSUE-3-314-319.pdf>
6. Poonam, Chauhan, R. S. (2013). Compression and Classification of Hyperspectral Images using an Algorithm based on DWT and NTD. *Advance in Electronic and Electric Engineering*, 3 (4), 447–456. Available at: http://www.ripublication.com/aeec/58_pp%20%20447-456.pdf
7. Vallakati, M. B., Sedamkar, R. R. (2012). Low Complexity DCT-based DSC approach for Hyperspectral Image Compression with Arithmetic Code. *IJCSI International Journal of Computer Science Issues*, 9 (5), 277–284. Available at: <https://docplayer.net/135044103-Low-complexity-dct-based-dsc-approach-for-hyperspectral-image-compression-with-arithmetic-code.html>
8. Keerthana, P., Sivasankar, A. (2013). The Impact of Lossy Compression on Hyperspectral Data Adaptive Spectral Unmixing and PCA Classification. *International Journal of Science and Modern Engineering*, 1 (7), 35–37. Available at: <https://www.ijisme.org/wp-content/uploads/papers/v1i7/G0340061713.pdf>
9. Mohand, O., Leila, A., Mourad, L., Soltane, A. (2012). Aviris Hyperspectral Images Compression Using 3d Spiht Algorithm. *IOSR Journal of Engineering*, 02 (10), 31–36. doi: <https://doi.org/10.9790/3021-021023136>
10. Aiazzi, B., Alparone, L., Baronti, S., Lastri, C., Selva, M. (2012). Spectral Distortion in Lossy Compression of Hyperspectral Data. *Journal of Electrical and Computer Engineering*, 2012, 1–8. doi: <https://doi.org/10.1155/2012/850637>
11. Liang, Y., Li, J., Guo, K. (2012). Lossless compression of hyperspectral images using hybrid context prediction. *Optics Express*, 20 (7), 8199. doi: <https://doi.org/10.1364/oe.20.008199>
12. Nian, Y., He, M., Wan, J. (2015). Lossless and near-lossless compression of hyperspectral images based on distributed source coding. *Journal of Visual Communication and Image Representation*, 28, 113–119. doi: <https://doi.org/10.1016/j.jvcir.2014.06.008>
13. Pizzolante, R., Carpentieri, B. (2014). Band Clustering for the Lossless Compression of AVIRIS Hyperspectral Images. *ACEEE Int. J. on Signal and Image Processing*, 5 (1), 1–14. Available at: <https://vdocuments.net/204498292-band-clustering-for-the-lossless-compression-of-aviris-hyperspectral.html>
14. Sarinova, A., Zamyatin, A. (2020). Methodology for Developing Algorithms for Compressing Hyperspectral Aerospace Images used on Board Spacecraft. *E3S Web of Conferences*, 223, 02007. doi: <https://doi.org/10.1051/e3sconf/202022302007>